

Application of laser scanning for automated efficiency assessment of solar panels: a case study in Uzbekistan

Shakhzod Takhirov¹, Sultan Kudratov², Akbar Normo'minov³, Zhamshid Takhirov⁴

¹Department of Civil and Environmental Engineering, University of California, Berkeley, California, U.S.A.

^{2,3}Department of Programming Technologies, Tashkent University of Information Technologies, Tashkent, Uzbekistan

⁴Sensor Fusion and Monitoring Technologies, LLC, Walnut Creek, California, U.S.A.

¹Corresponding author

E-mail: ¹takhirov@berkeley.edu, ²s.kudratov@gmail.com, ³normominovakbar@gmail.com,

⁴jtakhirov@gmail.com

Received 26 October 2025; accepted 20 November 2025; published online 22 December 2025

DOI <https://doi.org/10.21595/vp.2025.25705>



74th International Conference on Vibroengineering in Tashkent, Uzbekistan, November 27-29, 2025

Copyright © 2025 Shakhzod Takhirov, et al. This is an open access article distributed under the Creative Commons Attribution License, which permits unrestricted use, distribution, and reproduction in any medium, provided the original work is properly cited.

Abstract. This article presents an approach for automated assessment of the efficiency of pre-installed solar panel arrays. It is based on point clouds of large solar panel arrays distributed across space, with various orientations relative to the sun. As a typical example, without limiting the scope of application, a terrestrial laser scanner was used. Multiple buildings in a city block were laser-scanned to obtain the locations and orientations of the arrays. To demonstrate the developed approach, only one solar system on a building was considered in this study. The approach allows evaluating deficiencies in power production efficiency and comparing them with cost-effective modifications. The cost-benefit analysis can be performed based on this assessment. For future applications, the point clouds can be collected by other means, such as drones (for example).

Keywords: solar panel, renewable energies, optimal tilt, laser scanning, efficiency assessment, modeling.

1. Introduction

Solar energy is one of the most dynamically developing sectors of renewable energy [1, 2]. In the face of global climate change and rising energy consumption, countries are striving to utilize environmentally friendly energy sources. One key area of this process is the implementation of photovoltaic (PV) systems [3, 4].

The efficiency of solar panels depends on many factors: solar insolation, regional climate, the quality of the photovoltaic cells, and, most importantly, the panel tilt angle [3, 5]. For Uzbekistan, and particularly for Tashkent, solar energy has enormous potential. According to statistics, the country receives over 250 sunny days per year, and the average annual solar radiation level exceeds 1,600 kWh/m² [6]. This makes the republic one of the leaders in Central Asia in terms of solar power plant development potential [7].

There are a few commonly used approaches to determining the tilt angle of solar panels. The first approach is based on empirical formulas that assume the best tilt angle equals the location's latitude $\pm 10\text{--}15^\circ$ [5], [8]. The second approach is based on experimental observations, and the angle is selected based on long-term meteorological observations [9]. The third approach is based on mathematical modeling and predictions of the sun's location by using geometric and physical models of solar motion [1], [3], [6].

In addition, recent comparative analyses of fixed-tilt and tracking PV systems show that tracking configurations can improve annual energy yield by 15-25 %, depending on latitude and climatic zone [9], [10]. However, these systems are more expensive and require complex maintenance, so determining the optimal fixed tilt angle remains an important engineering task [10], [11].

The cost-benefit analysis, based on a review of the existing literature, is as follows. Based on the review of [9, 10, 16, 17], tracking systems are a sound investment in sunny regions – typically delivering 20-30 % more electricity output and lower lifetime cost per kWh than fixed-tilt systems. Based on [9, 16], single-axis trackers are the best value: simpler, cheaper, and close to dual-axis performance. They are widely used in utility-scale plants worldwide. In contrast, dual-axis trackers may suit special cases but are not cost-effective in general. It is well-known that solar panels become less efficient when their temperature exceeds a certain threshold. While solar panel cooling systems, such as spray-water designs, are possible and show promise in lab conditions, they are impractical for large-scale desert use without water recycling. In addition, cost-benefit analysis should include: (1) full-year performance data (not just day-level), (2) downtime and stow losses, (3) soiling and cleaning costs, (4) bifacial modules and reflective ground effects, and (4) hourly energy pricing and curtailment. When these are added, the realistic financial benefit of tracking typically equals 15-25 % more net revenue, rather than the optimistic 30 % headline.

This study focuses on one PV system installation in the New Uzbekistan area of Tashkent (Uzbekistan). Geographical and climatic Features of Tashkent are as follows: Tashkent is located at a latitude of 41.31°N and a longitude of 69.28°E . The time zone is UTC+5. A distinctive feature of the region is its pronounced continental climate. In winter, the sun rises low on the horizon, so the panels must be tilted at a steep angle to capture the sun's rays at right angles. In summer, on the contrary, the sun is high, and the panels must be positioned closer to the horizontal. It is worth noting that there are many roof-installed PV systems in Uzbekistan, and the majority of them are fixed-axis.

The main objective is to assess the efficiency of a typical PV system installation in Tashkent and to propose improvements if deficiencies are identified. The angular orientations of the solar panels in space were obtained by using a terrestrial laser scanner.

2. Point cloud of the solar panels

2.1. Laser scanning of a building block

As part of a large-scale efficiency assessment project of solar panels installed on the rooftops of several buildings, a set of newly constructed buildings in the New Uzbekistan area of Tashkent was laser-scanned. The laser scanning project was conducted on September 15, 2025, and included a few buildings around a small square. The terrestrial laser scanner RTC360 [12] from Leica Geosystems was used in this study. The scanning was conducted from multiple stations, and the final registration of the point clouds collected from different stations was done in Cyclone Register 360+ software package [13], also from Leica Geosystems. The resultant point cloud is shown in Fig. 1, with the intensity colors of the returned laser beam.

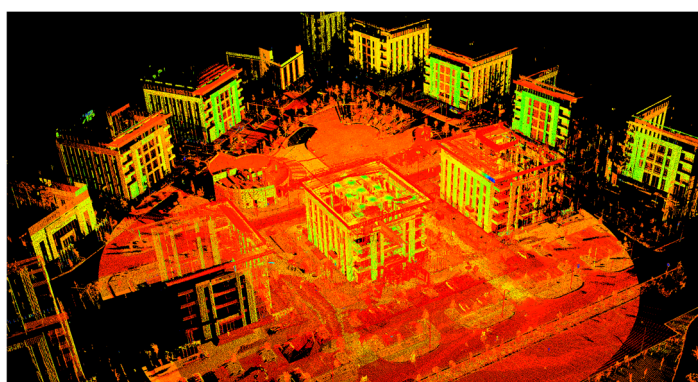


Fig. 1. Point clouds of newly constructed buildings with solar arrays on top

3. Point cloud of solar panel array and its analysis

One of the main objectives is to develop an approach for automated, mass-scale efficiency analysis of solar panel arrays based on the calculation of panel orientation from a laser scanner. As shown in Fig. 1, all the buildings have solar panels on their rooftops.

To demonstrate the developed approach, only one building was considered in this study. The point cloud of the building with an array of solar panels on top is shown in Fig. 2.

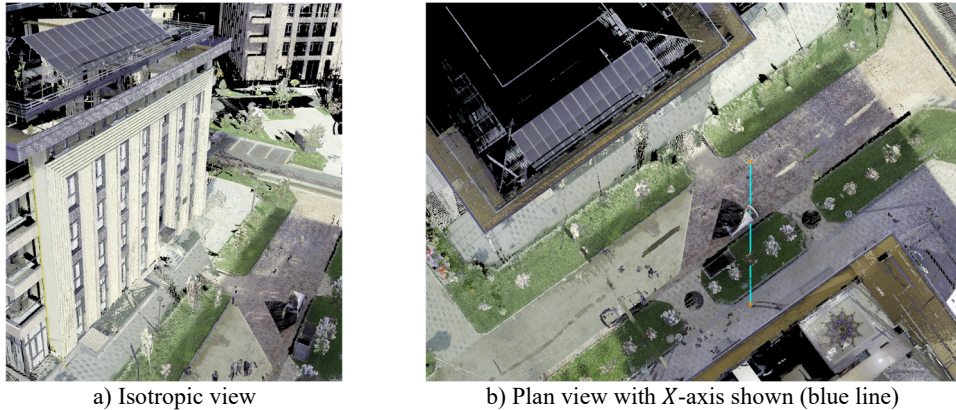


Fig. 2. Point cloud of the selected building

Based on the measurements conducted at the site, the building's south wall is oriented at 54 degrees to the north-east. The point cloud coordinate system was adjusted accordingly, and the resulting coordinate system is shown in Fig. 2(a) and Fig. 2(b). The latter images show the point cloud colored with the natural colors collected by the still-imaging camera built into the scanner.

Fig. 2(b) shows the *X*-axis of the new coordinate system, introduced to align it with magnetic north. In this plan view image, the *X*-axis is shown as a blue line, and its upward direction points north.

The point cloud of the solar panel array, isolated from the rest of the building, is presented in Fig. 3(a).

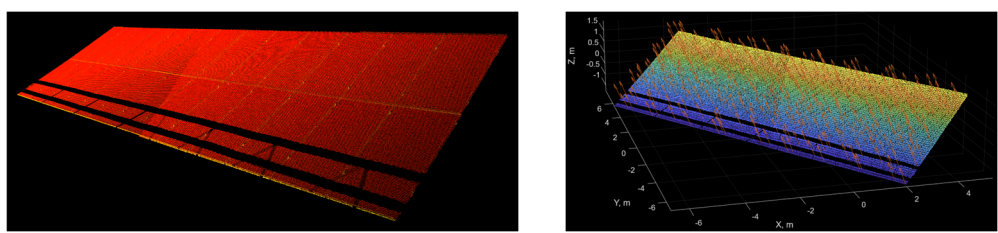


Fig. 3. Analysis of the point cloud of the solar panel array

The point cloud of the solar panel array was analyzed in MATLAB [14] environment. The normals to the point cloud were computed as shown in Fig. 3(b). This image was obtained as a result of the following. First, the point cloud was down-sampled to achieve an even point distribution. Second, a special MATLAB function that uses several neighboring points to generate a normal to the surface was used. In this paper, a hundred neighboring points were used. The degree of down-sampling and the number of neighboring points can be adjusted based on the point cloud's density.

Due to an error in acquiring the point clouds and some reflectivity-related issues, the point cloud contained some noise. All three components were checked for variability, and the coefficient

of variability (COV) was calculated for each component. The COV is the ratio of the standard deviation to the mean expressed as a percentage. It was determined that the first component has a COV of 2.9 %, the second component has a COV of 3.8 %, and the third component has a COV of 1.0 %. Since the COV did not exceed 45 for all three components, this variability was considered acceptable.

The angles of a normal vector with respect to the reference X -axis and Z -axis were obtained by computing the dot product (scalar product) of the normal vector with the unit vector of the respective axis, namely $(1,0,0)$ and $(0,0,1)$. These computations were conducted for the average values of X , Y , and Z components of the normal vectors. The results reveal that the angle to the X -axis is -144.2 degrees. In contrast, the normal inclination with respect to the vertical axis is 59.1 degrees, as presented in Fig. 4(a). This image also shows a round portion of the solar panel in the middle of the array where the origin of the coordinate system was selected.

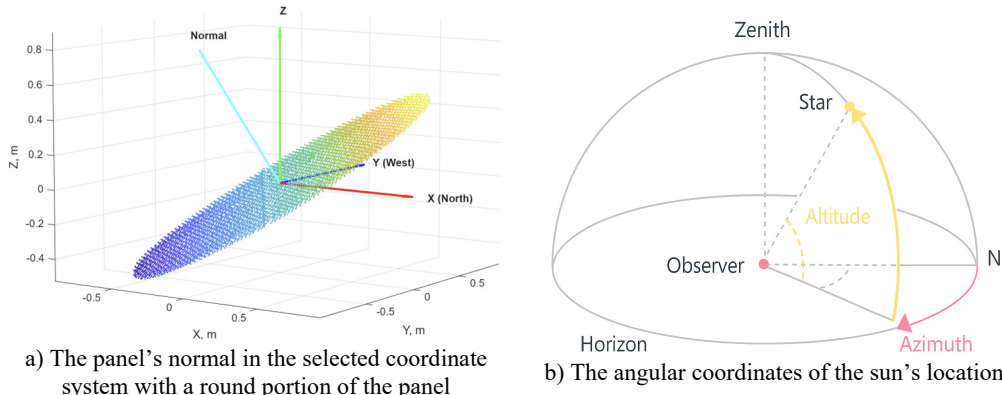


Fig. 4. The panel's normal and angular coordinates of the sun's location

The angular coordinates of the sun's location are shown in Fig. 4(b). Information on the sun's angular coordinates is widely available, including a few online calculators (see [15] as a representative example).

As an example, the change of the sun's location on the day of scanning, September 15, 2025, is presented in Fig. 5(a). This data was taken from [15] for the geo-location of the scanned site.

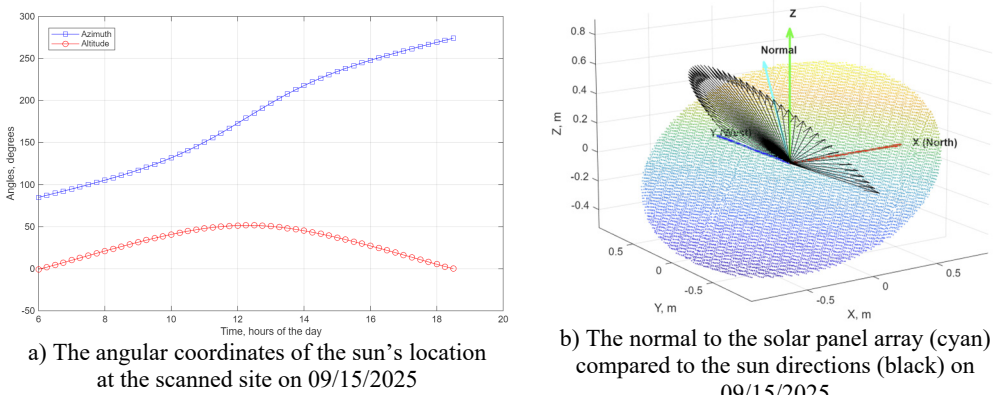


Fig. 5. The angular coordinates of the sun's location on 09/15/2025 and their vector representation

In the coordinate system of the sun depicted in Fig. 4(b), the azimuth of the solar panel is 144.2 degrees, and the altitude is 30.9 degrees (which is a result of subtracting 59.1 degrees from 90 degrees).

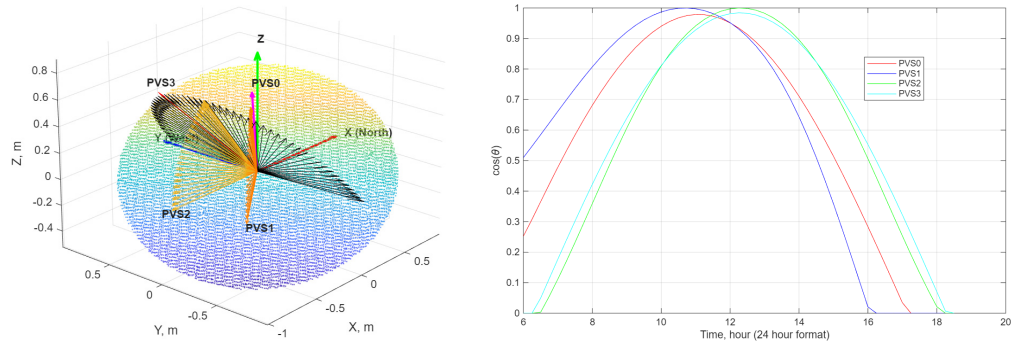
For this particular day, the normal of the solar panel array has a higher altitude than the maximum value of the sun's altitude, as shown in Fig. 5(b). In this figure, the sun directions on the day of scanning are shown as black arrows with 15-minute intervals.

To conduct a comparative study of the efficiency of this actual installation and potential modifications, four models were introduced, as listed in Table 1. It is worth noting that modifications PVS2 and PVS3 may result in a reduction in square footage. For simplicity of the discussion, this is ignored in this study and will be investigated in future research.

Table 1. Models of PV systems

Model	Description	Cost-related note
PVS0	This actual installation without any modifications	No cost
PVS1	The current PV system is modified into a single-axis system with a pivoting axis along the building	The least expensive
PVS2	The current PV system has been modified to a single-axis south-facing system with a pivoting axis along the building	More expensive option than SP01 and requires a loss of some energy for turning the panels
PVS3	The current PV system has been modified to a fixed south-facing system with a tilt equal to the latitude of the installation site	More expensive option than SP01, but does not require any controller or actuators to turn the panels

For PVS1 and PVS2, the normal to the solar panel array will vary throughout the day, as shown in Fig. 6(a), because each is a single-axis system. In contrast, PVS0 and PVS3 are fixed-axis systems, and as such, their normals remain fixed throughout the day.



a) The normals of all models compared to the sun directions (black) on 09/15/2025

b) The variation of this cosine function with time (as an example, the day of scanning is shown)

Fig. 6. The normals of all PV models and the resultant cosine function

The angle between the sun's direction and the normal to the solar panel array, θ , determines the array's power output, P :

$$P = P_{max} \cos(\theta). \quad (1)$$

The cosine of this angle can be obtained from the dot product (scalar product) of the unit normal vector, N_{panel} , and the unit vector pointing to the sun's current location, N_{sun} :

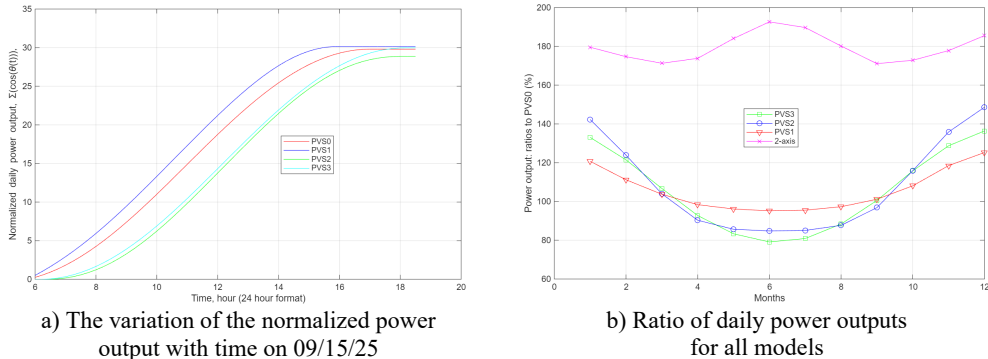
$$\cos(\theta) = N_{panel} \cdot N_{sun}. \quad (2)$$

From Eq (1), we can obtain that the variation of this cosine with time is the same as the variation of power over time, normalized by P_{max} :

$$\cos(\theta) = \frac{P}{P_{max}}. \quad (3)$$

This power variation over time is shown in Fig. 6(b). It is worth noting that the cosine can become negative, corresponding to cases when the sun is below the solar panel; as such, for these cases, the cosine is assumed to be zero.

Based on Eq. (3), the sum of all cosine variations throughout a day multiplied by the P_{max} will result in the power output of the solar panel. Therefore, this daily power output can be normalized by dividing by P_{max} , as shown in Fig. 7(b) for the same day. This image shows the cumulative sums of power output over time.



a) The variation of the normalized power output with time on 09/15/25

b) Ratio of daily power outputs for all models

Fig. 7. The variation of this normalized power output with time (as an example, the day of scanning is shown)

It is worth noting that the last number on the right side of each plot corresponds to the normalized daily electricity production, E_d/P_{max} , when multiplied by the time increment, dt (0.25 hours, which corresponds to 15 minutes), as presented below:

$$\frac{E_d}{P_{max}} = \frac{\Sigma P}{P_{max}} * dt = \Sigma \cos(\theta) * dt. \quad (4)$$

Plots similar to those presented for the day of laser scanning were generated for each month of 2025. The 15th day of each month was selected for that. All data were obtained from [15]. These daily power outputs were divided by those for the model PVS0, and the resulting ratios are presented in Fig. 7(b). As shown, all models with modifications to the current installation are more effective in the spring and fall months.

The numbers depicted in Fig. 11 were assumed to represent average monthly power outputs, and when multiplied by the number of days in each month, they produced the results shown in Table 2.

Table 2. Models of PV systems: annual normalized power output (2025)

Model	Annual normalized power output, E_d/P_{max}
PVS0	30,590.4
PVS1	31,937.8
PVS2	32,110.0
PVS3	31,385.8

The latter table shows that the current orientation and the fixed-axis configuration of the solar panel system are quite effective, as the system's production is close to that of all modified versions. The most effective one is the single-axis system oriented south. It is worth noting that the difference in the energy output is less dramatic than was expected from the cost-benefit analysis.

It is related to the fact that all these systems are idealized, and losses due to increased construction costs, actuator, controller, and other expenses are not yet accounted for. This will be done in the future extended study.

4. Conclusions

This article presents an approach for automated assessment of the efficiency of pre-installed solar panel arrays. It is based on the utilization of the laser scanner. The approach allows evaluating deficiencies in power production efficiency and comparing them with cost-effective modifications. The cost-benefit analysis can be performed based on this assessment.

Acknowledgements

The authors have not disclosed any funding.

Data availability

The datasets generated during and/or analyzed during the current study are available from the corresponding author on reasonable request.

Conflict of interest

The authors declare that they have no conflict of interest.

References

- [1] J. A. Duffie and W. A. Beckman, *Solar Engineering of Thermal Processes*. Wiley, 2013, <https://doi.org/10.1002/9781118671603>
- [2] S. Kalogirou, *Solar Energy Engineering: Processes and Systems*. Academic Press, 2014.
- [3] B. Y. H. Liu and R. C. Jordan, “The interrelationship and characteristic distribution of direct, diffuse and total solar radiation,” *Solar Energy*, Vol. 4, No. 3, pp. 1–19, Jul. 1960, [https://doi.org/10.1016/0038-092x\(60\)90062-1](https://doi.org/10.1016/0038-092x(60)90062-1)
- [4] C. Honsberg and S. Bowden, “Photovoltaics education website,” University of New South Wales, 2022.
- [5] J. Mas-Soler, E. Uzunoglu, G. Bulian, C. Guedes Soares, and A. Souto-Iglesias, “An experimental study on transporting a free-float capable tension leg platform for a 10 MW wind turbine in waves,” *Renewable Energy*, Vol. 179, pp. 2158–2173, Dec. 2021, <https://doi.org/10.1016/j.renene.2021.08.009>
- [6] I. Reda and A. Andreas, “Solar position algorithm for solar radiation applications,” *Solar Energy*, Vol. 76, No. 5, pp. 577–589, Jan. 2004, <https://doi.org/10.1016/j.solener.2003.12.003>
- [7] M. S. Khan, M. A. M. Ramli, H. F. Sindi, T. Hidayat, and H. R. E. H. Bouchekara, “Estimation of solar radiation on a PV panel surface with an optimal tilt angle using electric charged particles optimization,” *Electronics*, Vol. 11, No. 13, p. 2056, Jun. 2022, <https://doi.org/10.3390/electronics11132056>
- [8] A. R. Salih, “Seasonal optimum tilt angle of solar panels for 100 cities in the world,” *Al-Mustansiriyah Journal of Science*, Vol. 34, No. 1, pp. 104–110, Mar. 2023, <https://doi.org/10.23851/mjs.v34i1.1250>
- [9] K. Al-Rushadi and M. Al-Mosawi, “Comparative study with analysis of fixed-tilt and tracked solar photovoltaic panels,” in *8th International Conference on Green Energy and Applications (ICGEA)*, pp. 242–248, Mar. 2024, <https://doi.org/10.1109/icgea60749.2024.10560860>
- [10] M. R. Sharaby, S. W. Sharshir, A. A. Elbahoul, A. W. Kandeal, and M. Rashad, “Performance evaluation of fixed and sun-tracking photovoltaic systems integrated with spray cooling,” *Solar Energy*, Vol. 288, p. 113310, Mar. 2025, <https://doi.org/10.1016/j.solener.2025.113310>
- [11] T. Demirdelen, H. Alici, B. Esenboğa, and M. Güldürek, “Performance and economic analysis of designed different solar tracking systems for mediterranean climate,” *Energies*, Vol. 16, No. 10, p. 4197, May 2023, <https://doi.org/10.3390/en16104197>
- [12] “Leica RTC360 3D laser scanner.” Leica Geosystems AG, <https://leica-geosystems.com/products/laser-scanners/scanners/leica-rtc360>

- [13] “Cyclone Register 360.” Leica Geosystems AG, <https://rcdocs.leica-geosystems.com/cyclone-register-360/latest/help-cyclone-register-360>
- [14] “Matlab version R2025b,” The MathWorks, Inc., 2025.
- [15] “Solar data.” SunCalc, <https://www.suncalc.org>
- [16] A. Elahi Gol and M. Ščasný, “Techno-economic analysis of fixed versus sun-tracking solar panels,” *International Journal of Renewable Energy Development*, Vol. 12, No. 3, pp. 615–626, May 2023, <https://doi.org/10.14710/ijred.2023.50165>
- [17] M. Mahendran, “An experimental comparison between single-axis tracking and fixed photovoltaic panels,” University Malaysia Pahang, 2013.